

Correlation between structure and physical properties of chalcogenide glasses in the $\text{As}_x\text{Se}_{1-x}$ system

Guang Yang,^{1,2} Bruno Bureau,¹ Tanguy Rouxel,² Yann Gueguen,² Ozgur Gulbiten,³ Claire Roiland,¹ Emmanuel Soignard,⁴ Jeffery L. Yarger,⁴ Johann Troles,¹ Jean-Christophe Sangleboeuf,² and Pierre Lucas^{3,*}

¹UMR CNRS 6226 Sciences Chimiques, Groupe Verres et Céramiques, Université de Rennes I, Campus de Beaulieu, 35042 Rennes Cedex, France

²LARMAUR, ERL CNRS 6274, Université de Rennes I, Campus de Beaulieu, 35042 Rennes Cedex, France

³Department of Materials Science and Engineering, University of Arizona, 4715 E. Fort Lowell Road, Tucson, Arizona 85712, USA

⁴Department of Chemistry and Biochemistry, Arizona State University, Tempe, Arizona 85287-1604, USA

(Received 14 October 2010; published 17 November 2010)

Physical properties of chalcogenide glasses in the $\text{As}_x\text{Se}_{1-x}$ system have been measured as a function of composition including the Young's modulus E , shear modulus G , bulk modulus K , Poisson's ratio ν , the density ρ , and the glass transition T_g . All these properties exhibit a relatively sharp extremum at the average coordination number $\langle r \rangle = 2.4$. The structural origin of this trend is investigated by Raman spectroscopy and nuclear magnetic resonance. It is shown that the reticulation of the glass structure increases continuously until $x = 0.4$ following the "chain crossing model" and then undergoes a transition toward a lower dimension pyramidal network containing an increasing number of molecular inclusions at $x > 0.4$. Simple theoretical estimates of the network bonding energy confirm a mismatch between the values of mechanical properties measured experimentally and the values predicted from a continuously reticulated structure, therefore corroborating the formation of a lower dimension network at high As content. The evolution of a wide range of physical properties is consistent with this sharp structural transition and suggests that there is no intermediate phase in these glasses at room temperature.

DOI: [10.1103/PhysRevB.82.195206](https://doi.org/10.1103/PhysRevB.82.195206)

PACS number(s): 61.43.Dq, 81.05.Gc

I. INTRODUCTION

Chalcogenide glasses from the As—Se system have been studied for several decades due to their technological importance in infrared optics. These glasses possess good stability against crystallization and a wide transparency in the infrared domain which has made them the material of choice for technological development such as microstructured fibers¹ relief gratings,² or planar waveguides.³ Some of their physical properties such as thermodynamic and electrical have been investigated^{4,5} and several models for their structure have also been proposed^{6–13} although no consensus appears to have been reached.¹⁴ In addition these glasses have raised much interest due to their large photosensitivity and a variety of light-induced structural changes have been reported.^{15–17}

The structure of chalcogenide glasses is commonly described as a network of covalent bonds obeying the 8-N rule. Based on this assumption, Phillips and Thorpes have developed the rigidity percolation theory which compares the number of angular and bond constraints with the number of structural degrees of freedom and predicts that a structural threshold is reached for an average coordination value of $\langle r \rangle = 2.4$ corresponding to a topology where angular and bond constraints amount exactly to the degrees of freedom in the structure.^{18–20} This threshold is between an underconstrained floppy phase for $\langle r \rangle < 2.4$ and an overconstrained rigid phase for $\langle r \rangle > 2.4$. Senapati and Varshneya²¹ have reported that the glass-forming liquid at $\langle r \rangle = 2.4$ had minimum configurational energy and hence an optimum resistance to crystallization. This theory was extended using the concept of "self-organization" of the glassy network resulting in a structure that remains rigid but unstressed over a wider range of com-

positions near $\langle r \rangle = 2.4$.²² The unstressed domain between the floppy and rigid phase was then called the "intermediate phase."^{23–25} This phase was observed in the As—Se system using modulated differential scanning calorimetry and was explained by postulating the existence of As=Se double bonds⁸ but Golovchak *et al.*^{6,14,26} have since then debated their existence.

For Se-rich compositions in the range $0 < x < 0.4$, investigations with direct structural probe such as nuclear magnetic resonance (NMR) and x-ray photon spectroscopy (XPS) are in good agreement and indicate that the As—Se glass structure follows the "chain crossing model."^{6,10} In this model, chains of Se are progressively cross linked by As atom as x increases. However it is less clear how the glass structure evolves for As-rich composition in the range $0.4 < x < 0.6$ with x greater than the stoichiometric $\text{As}_{40}\text{Se}_{60}$. Following the constraint theory it could be expected that the structure follows a "continuous reticulation model" where a continuous glass network progressively become more and more overconstrained, however previous studies suggest otherwise.^{8,12} In this work, a set of physical properties including the elastic moduli, glass transition, and density were measured for a series of $\text{As}_x\text{Se}_{1-x}$ glasses and their structure was consecutively characterized by Raman and NMR. These results indicate a sharp structural transition at $\langle r \rangle = 2.4$ and a failure of the continuous reticulation model to the benefit of a "molecular glass model." A parallel is drawn between this structural evolution and the change in physical properties of the glass.

II. EXPERIMENT

$\text{As}_x\text{Se}_{1-x}$ glass rods of composition $x = 0, 0.10, 0.15, 0.20, 0.25, 0.30, 0.35, 0.40, 0.45, 0.50, 0.55$, and 0.60 were pre-

pared in evacuated fused silica ampoules using the melt-quenching method.¹⁰ High purity raw materials (99.999 wt %) were sealed in silica ampoules under vacuum and introduced in a rocking furnace. The ampoules were heated far above the liquidus to a temperature of 750 °C where the melt is highly fluid and were then rocked for 10 h in order to ensure a good homogenization of the liquid. In order to condense a maximum of vapor in the liquid, the temperature was reduced to 500 °C for 1 h. The ampoules were finally quenched in water and annealed below T_g . The glassy nature of the obtained glasses was confirmed by x-ray diffraction (XRD) analysis and the optical homogeneity was verified with a thermal-imaging camera. The compositions of as-made glasses were analyzed by energy-dispersive spectroscopy using a JEOL JSM 6301 electron microscope. All mechanical properties measurements were performed within 1 month of synthesis in order to avoid any effect of aging associated with long-term storage. The glass densities ρ were measured by the Archimedes method using deionized water as the immersion fluid. The elastic moduli were calculated from the measurements of the longitudinal, V_l , and transverse, V_t , ultrasonic wave velocities with a relative error better than $\pm 2\%$ using 10 MHz piezoelectric transducers. Young's modulus E , shear modulus G , bulk modulus K , and Poisson's ratio ν , were derived from the classical elasticity relationships,²⁷

$$E = \rho(3V_l^2 - 4V_t^2)/[(V_l/V_t)^2 - 1], \quad (1)$$

$$G = \rho V_t^2, \quad (2)$$

$$\nu = E/(2G) - 1, \quad (3)$$

$$K = E/[3(1 - 2\nu)]. \quad (4)$$

Differential scanning calorimetry (DSC) measurement (TA DSC Q20, TA Instruments, Castle, USA) was conducted at a heating rate of 10 K/min under a N_2 atmosphere at ambient pressure.

⁷⁷Se ($I=1/2$) magic-angle spinning (MAS) NMR experiments are performed on a Bruker Avance 300 spectrometer (7.1 T) operating at Larmor frequency of 57.3 MHz for ⁷⁷Se using a 4 mm double-resonance probe head. For the glasses, ⁷⁷Se MAS spectra are recorded using a rotor synchronized Hahn spin-echo sequence to refocus the magnetization and avoid distortion of the baseline. The spinning frequency is set to 15 kHz to average the chemical shift anisotropy and weak homonuclear dipolar coupling between Se atoms (expected to be weak because of the low natural abundance of ⁷⁷Se). Thus, the broadness of the lines is mainly due to the isotropic chemical shift distribution characteristic of the vitreous state. The Fourier transformation is done from the whole echo in order to increase the S/N ratio and to obtain directly absorption mode line shape. The experimental parameters are: 4 μs $\pi/2$ pulse duration, 30 s recycle time and a delay between pulses equal to 121 μs ($=1s/\nu_R - p_1/2 - p_2/2$, where ν_R is the spinning frequency, p_1 and p_2 are, respectively, the durations of the $\pi/2$ and π pulses). The chemical shift was calibrated with a saturated solution of Me_2Se in $CdCl_3$. Due to the low concentration and sensitiv-

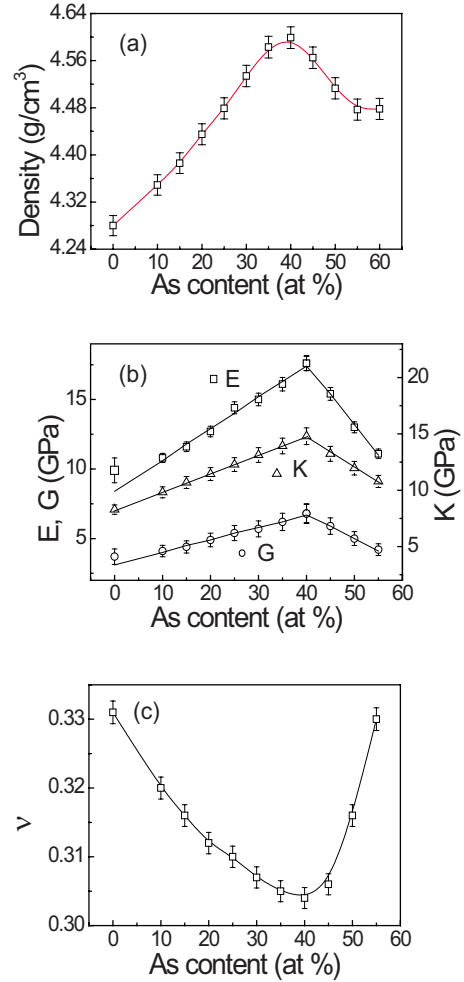


FIG. 1. (Color online) Composition dependence of the physical properties of As_xSe_{100-x} glasses. (a) Density ρ , (b) Young's modulus E , shear modulus G , bulk modulus K , and (c) Poisson's ratio ν .

ity of ⁷⁷Se, several thousand scans were accumulated and each spectrum was acquired over several days.

Raman spectra were acquired in 180° geometry with a 785 nm laser source. The laser power was controlled using neutral density filters. The laser was focused onto the sample using a 20× long working distance Mitutoyo objective with a numerical aperture of 0.42. The signal was discriminated from the laser excitation light using a Kaiser supernotch filter followed with a Shamrock edge filter. The data was collected using a Shamrock 303 Spectrograph and a deep depleted Andor charge-coupled detector. For each samples, spectra were first recorded at low intensity to ensure that no measurable changes due to photostructural effects took place during the measurement. The intensity and collection time were then progressively increased to optimize the signal-to-noise ratio while no visible spectral changes occurred.

III. RESULTS

A. Physical properties of As_xSe_{1-x} glasses

Figure 1 shows the compositional dependences of the glass density ρ over the whole glass forming domain $0 < x$

TABLE I. Experimental values of ν , K , U_{01} , V_0 , and $\langle r \rangle$ of $\text{As}_x\text{Se}_{1-x}$ glasses.

$\text{As}_x\text{Se}_{1-x}$	$\nu (\pm 0.005)$	$K (\pm 0.01)$ (GPa)	$V_0 (\pm 0.05)$ (cm^3/mol)	$U_{01} (\pm 0.1)$ (kJ/mol)	$\langle r \rangle$
0	0.331	8.28	18.45	152.8	2.00
0.10	0.320	9.82	18.06	177.3	2.10
0.15	0.316	10.69	17.86	190.9	2.15
0.20	0.312	11.44	17.62	201.5	2.2
0.25	0.310	12.28	17.40	213.7	2.25
0.30	0.307	13.13	17.15	225.1	2.30
0.35	0.305	13.93	16.92	235.7	2.35
0.40	0.304	14.80	16.82	248.8	2.4
0.45	0.306	13.23	16.90	223.6	2.45
0.50	0.316	11.96	17.05	203.8	2.5
0.55	0.330	10.78	17.14	184.8	2.55

<0.6 . The density increases in the range $0 < x < 0.4$ and then decreases in the range $0.4 < x < 0.6$ therefore showing a single minimum at $\langle r \rangle = 2.4$. Similarly, the measured values of Young's modulus E , shear modulus G , and bulk modulus K exhibit a sharp maximum at $\langle r \rangle = 2.4$ ($x = 0.40$) while Poisson's ratio ν exhibit a single minimum, at $\langle r \rangle = 2.4$.

It is known that the elastic moduli depend simultaneously on the interatomic bonding and on the atomic packing density. Indeed, the atomic bonding energy per mol atom is directly related to the bulk modulus and the atomic volume at equilibrium. In the simplistic case of a Mie-Coulomb potential, the first Grüneisen rule gives²⁸

$$K = m_1 n_1 U_0 / (9V_0), \quad (5)$$

where U_0 is the atomic bonding energy, V_0 is the atomic volume at equilibrium, and m_1 and n_1 are the exponents of the power law describing the attractive and the repulsive terms, respectively. V_0 can be estimated from the molar mass and the density ρ of the glass as shown in Table I. It is obviously difficult to transpose the concept of interatomic bond energy and atomic volume in the case of a multiconstituent glass for which structural data are rare and atomic volume are mostly unknown. However, assuming in a first approximation that $m_1 n_1 / 9 \approx 1$, which is not far from reality in chalcogen-rich chalcogenide glass,²⁹ interesting results can be obtained. As shown in Table I and Fig. 2, the mean atomic bonding energy $U_{0\text{ex}}$, derived from experimental elastic moduli and density data exhibits a linear dependence on As content along the two domains $0 \leq x \leq 0.40$ and $0.40 \leq x \leq 0.6$ with a maximum of 248.8 kJ/mol at $x = 0.40$. The $U_{0\text{ex}}$ data can be fitted with two lines expressed as: $U_{0\text{ex}} = 153.8 + 237.5x$ kJ/mol in the range $0 \leq x \leq 0.40$ and $U_{0\text{ex}} = 416.2 - 423.4x$ kJ/mol in the range $0.40 \leq x \leq 0.6$.

Alternatively, values for the mean atomic bonding energy can be independently obtained from the known interatomic bonding energy ($U_{\text{As-As}}$, $U_{\text{As-Se}}$, $U_{\text{Se-Se}}$) on the basis of simple structural assumption accounting for the stoichiometry. As shown in Fig. 3 there are three types of Se environments and four types of As environments in the $\text{As}_x\text{Se}_{1-x}$

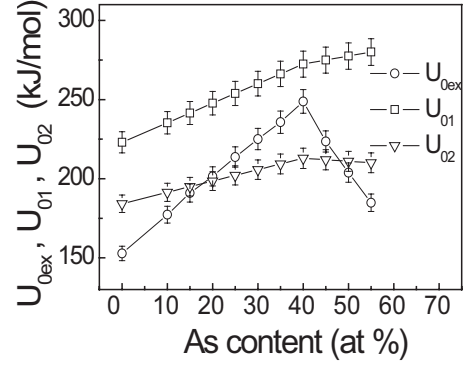


FIG. 2. Composition dependence of the mean atomic bonding energy $U_{0\text{ex}}$ obtained experimentally from K and V_0 compared with theoretical values predicted from a predicted from a continuously reticulated structure using bonding energies reported in Ref. 29 for U_{01} and Ref. 30 for U_{02} .

glassy system. Here we define the content of the corresponding Se and As units as: a_1 , b_1 , c_1 , d_1 , e_1 , f_1 , and g_1 in atomic percent. According to an ideal continuous reticulation model, for Se-rich compositions where $x < 0.25$, there are two types of Se atoms (**a** and **b**) and one type of As atom (**d**) (Fig. 3). Thus, for the range $0 \leq x < 0.25$, the mean atomic bonding energy can be obtained as

$$U_0 = a_1 \times 2 \times 0.5U_{\text{Se-Se}} + b_1 \times (0.5U_{\text{As-Se}} + 0.5U_{\text{Se-Se}}) + d_1 \times 3 \times 0.5U_{\text{As-Se}}. \quad (6)$$

Additionally, since there are only two kinds of Se and only one type of As the total content of Se and As can be written, respectively, as

$$a_1 + b_1 = 1 - x, \quad (7)$$

$$d_1 = x. \quad (8)$$

And since every **b**-type Se atom is linked to a **d**-type As atom, it derives that

$$b_1 = 3d_1. \quad (9)$$

So, Eq. (6) can be written as

$$U_0 = U_{\text{Se-Se}} + (3U_{\text{As-Se}} - 2.5U_{\text{Se-Se}})x. \quad (10)$$

Similarly, in the range $0.25 \leq x \leq 0.4$, there are two types of Se (**b** and **c**) and one type of As (**d**) in the sample. Thus, U_0 can be expressed as

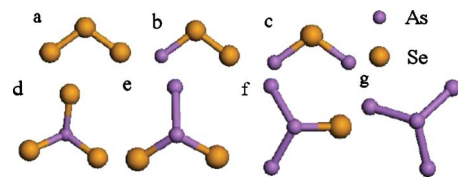


FIG. 3. (Color online) The three types of Se environments and four types of As environments possible in $\text{As}_x\text{Se}_{100-x}$ glasses. These seven environments labeled **a**, **b**, **c**, **d**, **e**, **f**, and **g** are used in the calculation of the mean atomic bonding energy U_0 .

$$U_0 = b_1 \times (0.5U_{\text{As-Se}} + 0.5U_{\text{Se-Se}}) + c_1 \times 2 \times 0.5U_{\text{As-Se}} + d_1 \times 3 \times 0.5U_{\text{As-Se}}. \quad (11)$$

Again, the content of As can be written as Eq. (8) and the content of Se can be written as

$$b_1 + c_1 = 1 - x. \quad (12)$$

And the relation between As and Se atomic content can be derived from Fig. 3 as

$$b_1 + 2c_1 = 3d_1. \quad (13)$$

So, Eq. (11) can be written as

$$U_0 = U_{\text{Se-Se}} + (3U_{\text{As-Se}} - 2.5U_{\text{Se-Se}})x, \quad (14)$$

which is the same as Eq. (10).

Finally, in the range $0.4 < x \leq 0.6$, according to the ideal continuous reticulation model, for As-rich compositions, there are only one type of Se (c) and up to four types of As (d, e, f, and g). Thus, U_0 can be expressed as

$$U_0 = c_1 \times 2 \times 0.5 \times U_{\text{As-Se}} + d_1 \times 3 \times 0.5 \times U_{\text{As-Se}} + e_1 \times (2 \times 0.5 \times U_{\text{As-Se}} + 0.5 \times U_{\text{As-As}}) + f_1 \times (0.5 \times U_{\text{As-Se}} + 2 \times 0.5 \times U_{\text{As-As}}) + g_1 \times 3 \times 0.5 \times U_{\text{As-As}}. \quad (15)$$

The content of As and Se atoms can be written as

$$d_1 + e_1 + f_1 + g_1 = x, \quad (16)$$

$$c_1 = 1 - x. \quad (17)$$

And the relation between As and Se atomic content can also be obtained as

$$3d_1 + 2e_1 + f_1 = 2c_1. \quad (18)$$

So, Eq. (11) can be written as

$$U_0 = 2U_{\text{As-Se}} - U_{\text{As-As}} + (2.5U_{\text{As-As}} - 2U_{\text{As-Se}})x. \quad (19)$$

In summary, if we assume an ideal continuous reticulation model the theoretical values of the mean atomic bonding energy U_0 follow two linear sections expressed as Eqs. (10) and (19) in the range $0 \leq x \leq 0.40$ and $0.40 \leq x \leq 0.6$, respectively. A quantitative estimate of U_0 can then be calculated based on experimental values of interatomic bonding energy obtained by calorimetry in Refs. 30 and 31. Based on the values reported in Ref. 30 $U_{\text{As-As}} = 202$ kJ/mol, $U_{\text{As-Se}} = 227$ kJ/mol, $U_{\text{Se-Se}} = 223$ kJ/mol the following theoretical results for mean atomic bonding energy are obtained: $U_{01} = 223 + 123.5x$ kJ/mol in the range $0 \leq x \leq 0.40$ and $U_{01} = 252 + 51x$ kJ/mol in the range $0.40 \leq x \leq 0.6$. Alternatively, based on the values reported in Ref. 31 $U_{\text{As-As}} = 134.39$ kJ/mol, $U_{\text{As-Se}} = 177.4$ kJ/mol, $U_{\text{Se-Se}} = 184.2$ kJ/mol the following values of U_0 are obtained: $U_{02} = 184.2 + 71.74x$ kJ/mol in the range $0 \leq x \leq 0.40$ and $U_{02} = 220.4 - 18.83x$ kJ/mol in the range $0.40 \leq x \leq 0.6$. Both estimates are plotted along with the experimentally derived values of U_0 in Fig. 2. It appears that there is a clear mis-

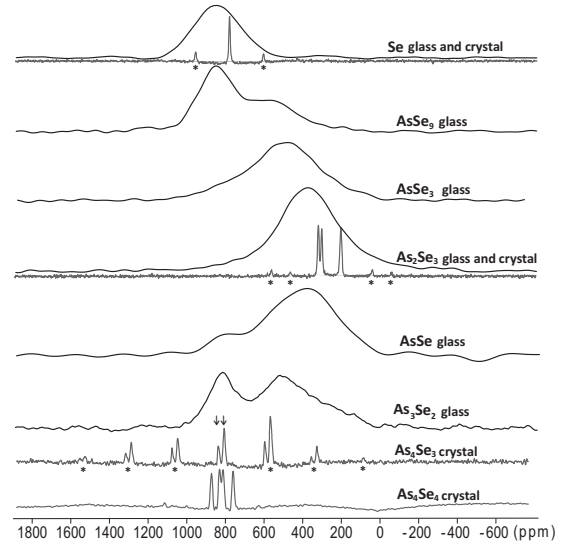


FIG. 4. ^{77}Se NMR MAS (15 kHz) spectra of amorphous Se, AsSe_9 , AsSe_3 , As_2Se_3 , AsSe , and As_3Se_2 shown with crystalline Se, As_2Se_3 , As_4Se_4 , and As_4Se_3 molecular crystals. The stars denote the spinning side bands and the arrows (for the As_4Se_3 spectrum) the lines which correspond to actual chemical sites.

match between the theoretical estimate and the experiment, especially in the $0.40 \leq x \leq 0.6$ range where the experimental U_0 shows a net decrease. This indicates a failure of the continuous reticulation model and suggests that the glass network experiences some dramatic changes at high As content, with possible formation of molecular fragments as previously suggested.^{8,12}

B. Structure of $\text{As}_x\text{Se}_{1-x}$ glasses

In order to identify the structural origin of the sharp extrema in physical properties at $\langle r \rangle = 2.4$, NMR and Raman spectroscopy were performed on the series of As—Se glasses. Figure 4 shows the NMR spectra of the Se, AsSe_9 , AsSe_3 , As_2Se_3 , AsSe , and As_3Se_2 samples. In the $0 < x < 0.4$ range, the spectra clearly indicate three distinct environments for ^{77}Se defined as **a**: Se—Se—Se, **b**: Se—Se—As, and **c**: As—Se—As. These spectra are in agreement with previous studies¹⁰ and are consistent with the “chains crossing model.” The pure Se glass shows a single peak at 850 ppm associated with the Se—Se—Se environment while the stoichiometric As_2Se_3 shows a single peak centered at 380 ppm associated with the As—Se—As environment. Instead the intermediate composition AsSe_3 shows a wide peak centered at 550 ppm which indicates a predominant distribution of Se—Se—As environment but also suggest the simultaneous existence of the two other environments. These spectra are consistent with the chain crossing model where “a” environments are progressively replaced by “b” and finally “c” environments as the arsenic content increases. The selenium chains cross-linking arsenic atoms become shorter and shorter until they eventually disappear. It is noted that the distribution of chains length deviates significantly from an *ideal* chain crossing model and that both short and long chains coexist. This description is consistent with

previous XPS (Ref. 6) and NMR (Ref. 10) studies.

Interestingly, the As-rich samples show a majority of As—Se—As environment along with a surprisingly large fraction of Se—Se—As and a notable contribution at 850 ppm which could have been assigned to Se—Se—Se but would not be consistent with the low Se content of these compositions. Indeed the NMR spectra of crystalline As_4Se_4 and As_4Se_3 show a strong signal in the same domain which rather suggests the presence of these molecular components in the glass. The As_4Se_3 and As_4Se_4 crystalline phases used for the NMR measurements were confirmed by both XRD and Raman. Note that both NMR spectra are in full agreement with the crystallographic data of these crystalline species. The As_4Se_4 cages contain four distinct Se with specific crystallographic features each of them giving rise to a specific NMR line. Similarly, each As_4Se_3 cage contains three Se, two of them being crystallographically equivalent. The As_4Se_3 NMR spectrum then exhibits two actual lines, one of them being twice as large as the other. These two lines are denoted by arrows in Fig. 4, the other lines denoted by stars correspond to the spinning side bands due to the magic-angle spinning and will average out in the glass. These results emphasize the ability of ^{77}Se NMR to accurately resolve structural information in solid state materials. The presence of these As-rich molecules in the glasses is also consistent with the relative intensities of the NMR peaks. Indeed the presence of large fractions of Se—Se—As fragments requires the presence of As-rich clusters in order to compensate for the Se-poor stoichiometry. Overall, the NMR interpretation indicates that the structure follows the chains crossing model in the range $0 < x < 0.40$ but subsequently loses its network reticulation and generates As-rich cage molecules in the range $0.40 < x < 0.6$. The reconstructed NMR spectra of the AsSe and As_3Se_2 glasses (not shown) indicate that 20% and 40%, respectively, of Se atoms are involved in such molecules in the glass structure.

The Raman spectra shown in Fig. 5 largely confirm this interpretation. In the Se-rich region, the Se chain mode at 255 cm^{-1} continuously decrease while the pyramidal AsSe_3 modes near 230 cm^{-1} simultaneously grow. But more interestingly the As-rich spectra clearly indicate the presence of very sharp features indicative of As_4Se_4 and As_4Se_3 molecular units. The deconvolution of the $\text{As}_{60}\text{Se}_{40}$ Raman spectra shown in Fig. 5(b) reveals the presence of sharp modes associated with As_4Se_4 at 206 cm^{-1} and 247 cm^{-1} (Ref. 32) and with As_4Se_3 at 198 , 236 , and 278 cm^{-1} .³³ These molecules are well characterized^{34,35} and have been previously observed in As—Se glasses by Raman¹⁶ and nuclear quadrupole resonance.¹² Another striking feature of these Raman spectra is a sharp and intense peak at 200 cm^{-1} which grows continuously with increasing arsenic content. This feature is characteristic of amorphous elemental arsenic.³⁶ The sharpness of the peak suggests that this mode is associated with As_4 tetrahedral units isostructural to P_4 molecules in white phosphorus. Density-functional studies have shown that these molecules are very stable³⁷ and their presence have previously been postulated in As-rich As—Se glasses.³⁸

In order to quantify this structural evolution Fig. 6 shows the results of the deconvolution of all the Raman spectra. All spectra were deconvoluted using known peak

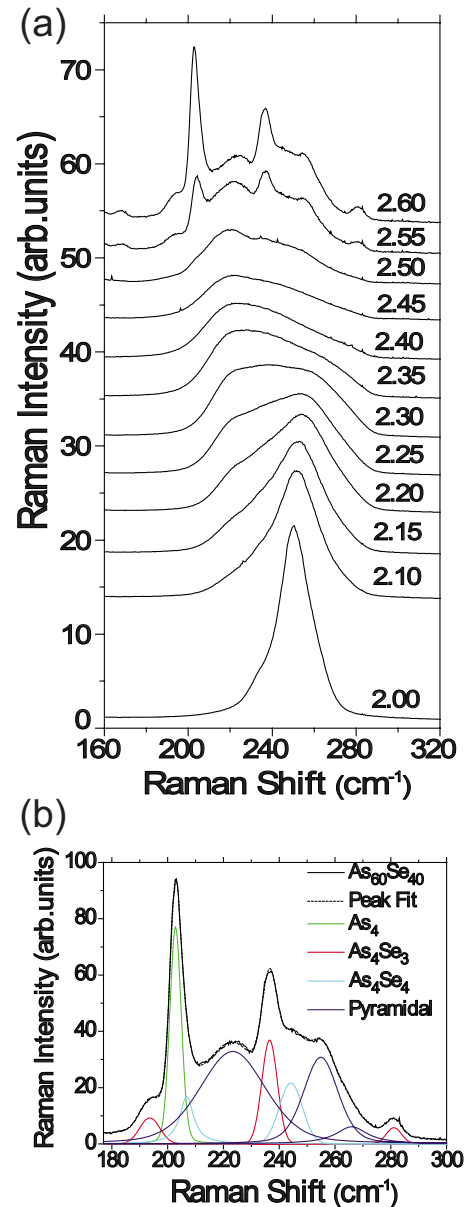


FIG. 5. (Color online) (a) Evolution of the Raman spectra in the $\text{As}_x\text{Se}_{100-x}$ glass system. (b) Example of spectral deconvolution for the $\text{As}_{60}\text{Se}_{40}$ sample.

assignments.^{9,32,33,36,39,40} The peak surface was integrated for the Se-chain modes and the As_4Se_4 , As_4Se_3 , and As_4 molecular modes. The plot of Fig. 6 shows a linear decrease in the Se-chain modes until it disappears at $x=0.4$ at which points the As_4Se_4 , As_4Se_3 , and As_4 molecular modes start to grow also linearly. It is interesting to note that the shape of this curve is reminiscent of the composition dependence of the physical properties shown in Fig. 1. Furthermore, the intensity and peak position of the AsSe_3 pyramidal mode was plotted as a function of composition in Fig. 7. Both curves also show a V shape reminiscent of the physical properties dependence.

It should be noted that the presence of As-rich molecular units revealed by Raman is in good agreement with the existence of large fraction of Se-rich Se—Se—As fragments

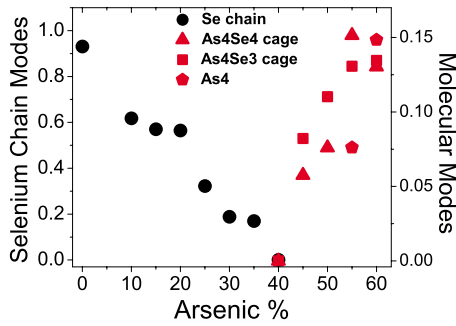


FIG. 6. (Color online) Quantitative results of the deconvolution of Raman spectra for As_xSe_{100-x} glasses. The Raman intensities for each modes, Se chains and As_4Se_4 , As_4Se_3 cage molecules were obtained by integrating the Raman peaks and normalized to the overall spectra.

observed by ^{77}Se NMR in $As_{50}Se_{50}$ and $As_{60}Se_{40}$. The structure of As-rich glasses can then be described as a backbone of $AsSe_3$ pyramid interconnected by Se atoms or Se—Se fragments and surrounded by As-rich molecular units. The evolution of this pyramidal backbone is consistent with the shift in $AsSe_3$ mode frequency observed in Fig. 7. Indeed it was shown that the position of the $AsSe_3$ mode is related to the apex angle of the pyramidal unit.⁹ It is shown here that this angle is maximum in the chemically ordered As_2Se_3 composition where every As is linked by a single Se atom. The apex angle then decreases on either side of the stoichiometric As_2Se_3 composition as the pyramidal units are linked by longer fragments, allowing more flexibility to the backbone.

IV. DISCUSSION

As shown in Fig. 1 the mechanical properties of the As—Se glass all show a relatively sharp extrema at $\langle r \rangle = 2.4$. These mechanical properties are typically a reflection of the bonding energy and the network reticulation. In particular, Poisson’s ratio ν is the negative of the ratio of the transverse contraction strain to longitudinal extension strain in the direction of elastic loading. Hence, it reflects the resistance that a material opposes to volume change respective to its shape and is small for shear-resistant compressible ma-

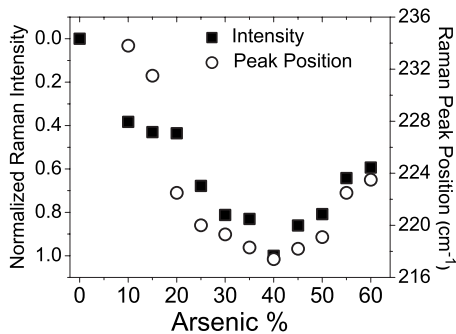


FIG. 7. (a) Composition dependence of the normalized intensity and the peak position of the main symmetric $AsSe_3$ pyramidal mode in As_xSe_{100-x} glasses.

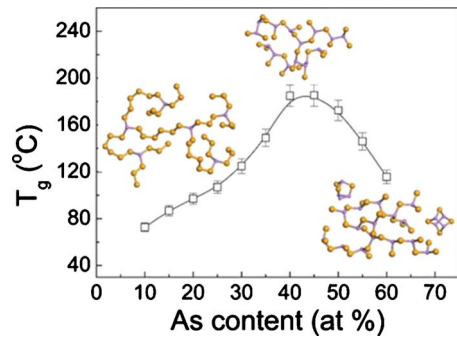


FIG. 8. (Color online) Composition dependence of the glass transition T_g in As_xSe_{100-x} glasses. The insets show the evolution of the structure with compositions.

terials. A remarkable correlation was observed between ν and the glass network connectivity.⁴¹ ν was found in various glass systems to decrease monotonically with an increase in the network cross linking. Since from simple theoretical consideration (Sec. III A), both the volume density of energy and the average coordination increase with the As content, both K and ν are expected to change monotonically with the As content. However our experimental investigations show that this is not the case. K is maximum and ν is minimum at $x=0.40$. The mean network bonding energy derived from K is also maximum at $x=0.40$. The continuous reticulation model assumed in Sec. III A therefore fails to explain the mechanical behavior of the glass because it does not account for possible clustering effect and ignores the role of the weak intermolecular van der Waals forces. The formation of molecular clusters revealed by spectroscopy decreases the network connectivity and the relatively weak intermolecular forces favor shear and lead to an increase in ν at high As content, although the average number of bonds per atom $\langle r \rangle$ keeps increasing. In other words, the system behaves more and more like a molecular liquid.

In summary, the structure of As_xSe_{1-x} glasses evolve from a one-dimensional (1D) to a two-dimensional (2D) network in the range $0 < x < 0.40$ following the chains crossing model and then evolve from two dimensions toward a zero-dimensional (0D) molecular glass for $x > 0.4$. This evolution is consistent with the change in K and ν , as well as density ρ . For $x \leq 0.40$, the density values increase regularly with the concentration of arsenic from 4.28 g cm^{-3} (g-Se) to 4.60 g cm^{-3} (A-Se) all showing that the shorter the chains, the higher the rigidity and compactness of the network. Then, for $x > 0.40$ the appearance of arsenic-rich molecular-like domains relieves the stress building up as the average coordination number increases and lead to a lower dimensionality and lower density network. Figure 8 shows that the glass transition T_g , which directly relate to the net link energy is fully consistent with this description. For $x < 0.40$ the energy required to break interchain van der Waals forces is small and the T_g is low while at $x=0.4$ the fully reticulated network requires breaking higher energy covalent bonds and the T_g is maximum. Then at $x > 0.4$ the T_g decrease again as the energy require to break intermolecular van der Waals forces become smaller again.

This analysis ignores the possibility that has recently been suggested that a significant fraction of arsenic atoms may be

fourfold coordinated in these glasses.⁸ The presence of these peculiar structural units was postulated in order to rationalize the observation of an intermediate phase where the structure is rigid but unstressed over a wide range of compositions in the As—Se system. This intermediate phase was derived by monitoring the enthalpy relaxation process of the structure while heating above T_g with a modulated DSC (MDSC).⁸ However it is shown here that a wide variety of physical properties measured on the low-temperature solid glasses show a single extrema at $\langle r \rangle = 2.4$. These sharp extrema are also consistent with the structural information collected at room temperature by NMR and Raman. This tends to indicate that the observation of the intermediate phase in $\text{As}_x\text{Se}_{1-x}$ glasses might be an artifact of the MDSC measurement performed at high temperature across the glass transition region where part of the network bonds are already broken and the number of network constraints is lower than in the glassy state at room temperature. Indeed, measurements performed at room temperature where the network is intact show no such intermediate phase and therefore do not require the existence of fourfold-coordinated arsenic atoms. The dependence of network constraints on temperature was recently demonstrated by Smedskjaer *et al.*⁴² in soda lime borate glasses. It was shown that a discrete temperature dependence of topological constraints could enable an analytical derivation of the composition dependence of hardness. Different topological constraints are lost at increasing temperature depending on their bond strength. This suggests that the intermediate phase observed in the region above T_g in $\text{As}_x\text{Se}_{1-x}$ glasses might be a reflection of the temperature dependence of structural constraints rather than the number of constraints in the room-temperature glass.

V. CONCLUSIONS

It is shown that the composition dependence of, E , G , K , ν , ρ , and T_g exhibit an extremum at $\langle r \rangle = 2.4$ in binary $\text{As}_x\text{Se}_{1-x}$ glasses. This trend indicates a dramatic structural change at $x=0.4$ which is confirmed by Raman and NMR spectroscopy. Indeed the glass network evolves from a 1D chain structure to a 2D pyramidal network in the range $0 < x < 0.4$ and then transitions to a lower dimension structure composed of a pyramidal backbone containing an increasing number of 0D molecular inclusions in the range $0.4 < x < 0.6$. This transition has a direct effect on the mechanical properties of these glasses and in particular Poisson's ratio which is known to correlate with the connectivity of the glass network.⁴¹ A wide variety of physical properties exhibit a single sharp extremum at $x=0.4$ therefore indicating that there is no intermediate phase in these glasses.

ACKNOWLEDGMENTS

Y.G. thanks the French Ministry of Research (Grant No. 25094-2007). P.L. thanks NSF-DMR under Grant No. 0806333 and NSF-ECCS under Grant No. 0901069 and the CNRS International Associated Laboratory for Materials & Optics. J. Yarger and E. Soignard would like to acknowledge support by the NNSA CDAC Grant No. DE-FC52-08NA28554 and by EFree, an Energy Frontier Research Center funded by the U.S. Department of Energy, Office of Science, Office of Basic Energy Sciences under Award No. DE-SC0001057.

*Corresponding author; pierre@u.arizona.edu

- ¹Q. Coulombier, L. Brilland, P. Houizot, T. Chartier, T. N. N'Guyen, F. Smektala, G. Renversez, A. Monteville, D. Méchin, T. Pain, H. Orain, J.-C. Sangleboeuf, and J. Trolès, *Opt. Express* **18**, 9107 (2010).
- ²C. Florea, J. S. Sanghera, L. B. Shaw, V. Q. Nguyen, and I. D. Aggarwal, *Mater. Lett.* **61**, 1271 (2007).
- ³N. Hô, M. C. Phillips, H. Qiao, P. J. Allen, K. Krishnaswami, B. J. Riley, T. L. Myers, and N. C. Anheier, Jr., *Opt. Lett.* **31**, 1860 (2006).
- ⁴T. Wagner and S. O. Kasap, *Philos. Mag. B* **74**, 667 (1996).
- ⁵J. Li, D. A. Drabold, S. Krishnaswami, G. Chen, and H. Jain, *Phys. Rev. Lett.* **88**, 046803 (2002).
- ⁶R. Golovchak, A. Kovalskiy, A. C. Miller, H. Jain, and O. Shpotyuk, *Phys. Rev. B* **76**, 125208 (2007).
- ⁷J. C. Mauro and A. K. Varshneya, *J. Non-Cryst. Solids* **353**, 1226 (2007).
- ⁸D. G. Georgiev, P. Boolchand, and M. Micoulaut, *Phys. Rev. B* **62**, R9228 (2000).
- ⁹S. Onari, O. Sugino, M. Kato, and T. Arai, *Jpn. J. Appl. Phys., Part 1* **21**, 418 (1982).
- ¹⁰B. Bureau, J. Troles, M. LeFloch, F. Smektala, G. Silly, and J. Lucas, *Solid State Sci.* **5**, 219 (2003).
- ¹¹V. Kovanda, M. Vlcek, and H. Jain, *J. Non-Cryst. Solids* **326–327**, 88 (2003).
- ¹²E. Ahn, G. A. Williams, and P. C. Taylor, *Phys. Rev. B* **74**, 174206 (2006).
- ¹³R. Golovchak, O. Shpotyuk, A. Kozdras, B. Bureau, M. Vlcek, A. Ganjoo, and H. Jain, *Philos. Mag.* **87**, 4323 (2007).
- ¹⁴R. Golovchak, H. Jain, O. Shpotyuk, A. Kozdras, A. Saiter, and J.-M. Saiter, *Phys. Rev. B* **78**, 014202 (2008).
- ¹⁵K. Antoine, H. Jain, M. Vlcek, S. D. Senanayake, and D. A. Drabold, *Phys. Rev. B* **79**, 054204 (2009).
- ¹⁶P. Krecmer, A. Sklenar, M. Vlcek, and S. R. Elliott, *Phys. Rev. B* **63**, 104201 (2001).
- ¹⁷A. V. Kolobov, V. A. Bershtein, and S. R. Elliott, *J. Non-Cryst. Solids* **150**, 116 (1992).
- ¹⁸M. F. Thorpe, *J. Non-Cryst. Solids* **57**, 355 (1983).
- ¹⁹J. C. Phillips and M. F. Thorpe, *Solid State Commun.* **53**, 699 (1985).
- ²⁰J. C. Phillips, *J. Non-Cryst. Solids* **34**, 153 (1979).
- ²¹U. Senapati and A. K. Varshneya, *J. Non-Cryst. Solids* **185**, 289 (1995).
- ²²M. F. Thorpe, D. J. Jacobs, M. V. Chubynsky, and J. C. Phillips, *J. Non-Cryst. Solids* **266–269**, 859 (2000).
- ²³C. Massobrio, M. Celino, P. S. Salmon, R. A. Martin, M. Micoulaut, and A. Pasquarello, *Phys. Rev. B* **79**, 174201 (2009).
- ²⁴P. Boolchand, X. Feng, and W. J. Bresser, *J. Non-Cryst. Solids*

- 293-295**, 348 (2001).
- ²⁵M. Micoulaut and J. C. Phillips, *Phys. Rev. B* **67**, 104204 (2003).
- ²⁶R. Golovchak, O. Shpotyuk, and A. Kozdras, *Phys. Lett. A* **370**, 504 (2007).
- ²⁷C. Bernard, V. Keryvin, J.-C. Sangleboeuf, and T. Rouxel, *Mech. Mater.* **42**, 196 (2010).
- ²⁸*Physical Properties of Solid Materials*, edited by C. Zwikker (Wiley Interscience, New York, 1954), p. 90.
- ²⁹T. Rouxel, *C. R. Mec.* **334**, 743 (2006).
- ³⁰E. V. Shkol'nikov, *Sov. J. Glass Phys. Chem.* **11**, 40 (1985).
- ³¹L. Pauling, *The Nature of the Chemical Bond* (Cornell University Press, Ithaca, NY, 1960).
- ³²W. Bues, M. Somer, and W. Brockner, *Z. Naturforsch. C* **35**, 1063 (1980).
- ³³W. Bues, M. Somer, and W. Brockner, *Z. Anorg. Allg. Chem.* **499**, 7 (1983).
- ³⁴R. Blachnik and U. Wickel, *Thermochim. Acta* **81**, 185 (1984).
- ³⁵R. Blachnik, *Thermochim. Acta* **213**, 241 (1993).
- ³⁶J. S. Lannin, *Phys. Rev. B* **15**, 3863 (1977).
- ³⁷P. Ballone and R. O. Jones, *J. Phys. Chem.* **100**, 4941 (1994).
- ³⁸P. Nagels, R. Callaerts, M. Van Roy, and M. Vlcek, *J. Non-Cryst. Solids.* **138-137**, 1001 (1991).
- ³⁹M. Ystenes, W. Brockner, and F. Menzel, *Vib. Spectrosc.* **5**, 195 (1993).
- ⁴⁰S. N. Yannopoulos and K. S. Andrikopoulos, *J. Chem. Phys.* **121**, 4747 (2004).
- ⁴¹T. Rouxel, H. Ji, T. Hammouda, and A. Moreac, *Phys. Rev. Lett.* **100**, 225501 (2008).
- ⁴²M. M. Smedskjaer, J. C. Mauro, and Y. Yue, *Phys. Rev. Lett.* **105**, 115503 (2010).